Marine Micropaleontology 186 (2024) 102319

Contents lists available at ScienceDirect

Marine Micropaleontology

journal homepage: www.elsevier.com/locate/marmicro

Holocene paleo-redox conditions in a microbial dolomitic lake using benthic foraminifera as bioindicators

Daniel François [a,1], Camila Areias [a,b], Nayara Dornelas [a], Luiz G.R. Sá-Valle [a,c], Anna Paula Soares Cruz [d], José Carlos Sícoli Seoane [e], Crisógono Vasconcelos [f], Nicolás M. Stríkis [g], Daniel Souza dos Santos [g], Adina Paytan [h], Cátia F. Barbosa [a,*]

[a] Programa de Pós-graduação em Geoquímica, Universidade Federal Fluminense, Outeiro de São João Batista, s/n, Centro, Niterói, Rio de Janeiro, CEP 24.020-141, Brazil
[b] Earth Sciences Department, Vrije Universiteit Amsterdam, Netherlands
[c] Departamento de Geologia e Geofísica, Universidade Federal Fluminense Niterói, Rio de Janeiro CEP 24.210-346, Brazil
[d] Department of Geological Sciences, California State University Bakersfield, 9001 Stockdale Highway, Bakersfield, CA 93311-1022, USA
[e] Laboratório Geodiversidade e Memória da Terra e Programa de Pós-graduação em Geologia, Universidade Federal do Rio de Janeiro, Rio de Janeiro, CEP 21.941-916, Brazil
[f] Centro de Desenvolvimento Tecnológico, Núcleo de Inovação e Tecnologia do Serviço Geológico do Brasil, RJ-22290-180 Rio de Janeiro, Brazil
[g] Instituto de Geociências, Universidade de São Paulo, Rua do Lago, 562, Cidade Universitária, São Paulo, SP 05508-090, Brazil
[h] Institute of Marine Science, University of California Santa Cruz, Santa Cruz, CA 95064, USA

ARTICLE INFO

Keywords:
Foraminifera test pore
Microbial mat
Oxygenation
Dolomite
Stable isotopes

ABSTRACT

Brejo do Espinho coastal lake (LBE) is one of the few places in the world where dolomite [$CaMg(CO_3)_2$] is precipitating in the modern environment under microbially induced processes and low oxygen conditions. We use pore morphometry of the foraminifera *Ammonia* cf. *A. veneta* to evaluate paleo-O_2 dynamics during the dolomitic depositional phase that took place at LBE in the late Holocene. Foraminiferal community structure was also investigated, and results were compared to bulk isotopic composition of carbonates, total organic carbon (TOC), and X-ray Diffraction of sediments (XRD). The correlation matrix (Spearman method) showed that *Ammonia* test pores morphometric parameters displayed significant correlations with overall biotic and geochemical data, with pore area presenting a relatively higher association. *Ammonia* test pores were primarily controlled by the degradation of organic matter (Pore area-TOC, $r = -0.84$), and foraminifera density appeared to be influenced by oxygen changes, with a higher abundance in the highest porosity intervals (Pore area-N, $r = 0.82$), indicating a direct effect of oxygen penetration on species dominance. These data also reveal a tolerant behavior of the low-O_2 bioindicator species *Quinqueloculina laevigata* and *A. veneta*. Understanding microbe-mineral interactions is critical for interpreting paleo records, and our data provide strong support for coupling assemblage and pores analysis as paleo-O_2 bioindicators for paleo-redox coastal settings.

1. Introduction

Foraminifera are valuable bioindicators due to their sensitivity to environmental changes, short lifespans, and widespread distribution (Murray, 2006). Their tests, with diverse morphophysiological adaptations, serve as important proxies for reconstructing past environments (Murray, 2006). Among test features, foraminiferal test pores are vital for respiration, responding to water oxygen levels. Some hyaline, perforated species, exhibit higher porosity and bigger pore size in oxygen-poor waters (Petersen et al., 2016; Rathburn et al., 2018; Lu et al., 2021), conditions in which clusters of mitochondria are also recognized to occur near the pore's termination (Leutenegger and Hansen, 1979; Bernhard and Sen Gupta, 1999). This association to O_2-dynamics has been studied and recently suggested to be controlled by metabolic and mechanical constraints of the foraminiferal tests (Sen Gupta and Machain-Castillo, 1993; Bernhard and Sen Gupta, 1999; Koho et al., 2018; Rathburn et al., 2018; Richirt et al., 2019b).

Due to a direct correlation with O_2, recent quantitative protocols

* Correspondence author.
E-mail address: catiafb@id.uff.br (C.F. Barbosa).
[1] Present address: Department of Ocean Systems, NIOZ Royal Netherlands Institute for Sea Research and Utrecht University, Texel, the Netherlands

https://doi.org/10.1016/j.marmicro.2023.102319
Received 1 July 2023; Received in revised form 15 November 2023; Accepted 20 November 2023
Available online 26 November 2023

based on pore morphometry were designed for robust analysis of deoxygenation conditions, important for monitoring the increase of O_2 minimum zones (e.g., Petersen et al., 2016; Tetard et al., 2017; Rathburn et al., 2018; Giordano et al., 2019). By displaying robustness and broad applicability, such protocols can be extended to improve the understanding of natural processes linked to oxygen availability, such as microbial induced carbonate precipitation, which is relevant to carbon sequestration and other oceanographical/geological processes.

In evidence, dolomite is a carbonate mineral [$CaMg(CO_3)_2$] that is rarely precipitated in modern environments (McKenzie and Vasconcelos, 2010). Brejo do Espinho (LBE), however, is a hypersaline lake in Brazil, where microbial communities play an important role in overcoming kinetic barriers to dolomite precipitation at surface temperature conditions (Bahniuk et al., 2015; Sánchez-Román et al., 2009). Modern dolomite-forming environments are primarily represented by hypersaline systems, such as coastal sabkhas, coastal lagoons, evaporative lakes, and alkaline lakes (Bontognali et al., 2010; Sanz-Montero et al., 2019; Shiraishi et al., 2023; Vasconcelos and McKenzie, 1997), as well as hemipelagic sediments on continental margins (Meister et al., 2007) and marine cold-seeps (Tong et al., 2019). As important archives, the lake sediments have been used to investigate modern dolomite precipitation process and elucidate geochemical conditions triggering dolomite formation (Areias et al., 2022; Nascimento et al., 2019), possibly analog to massive dolomite deposits in the geological record (Burns et al., 2000; McKenzie and Vasconcelos, 2008; Sánchez-Román et al., 2008). So far, studies in this field have underlined the importance of microbial communities (Vasconcelos and McKenzie, 1997; Warthmann et al., 2000, Warthmann et al., 2005; Van Lith et al., 2003; Vasconcelos et al., 2006; Sánchez-Román et al., 2008, 2009) and semi-arid climate (e.g., high evaporation, Mg/Ca ratio, salinity, and pH) for dolomite formation (Van Lith et al., 2002; Bahniuk et al., 2015; Nascimento et al., 2019), including the influence of a local upwelling system (Areias et al., 2022), which has redox conditions not yet elucidated.

Here we investigated deoxygenation patterns in the LBE sedimentological record over the last ~1.6 ka by accurately measuring surface morphometric pore parameters in specimens of *Ammonia* cf. *A. veneta* (Hayward et al., 2021), and studying the foraminiferal communities.

2. Study site

The formation of the Rio de Janeiro state coastal plain started around 123 kyr BP, during the last Pleistocene marine transgression (Barbosa, 1997; Turcq et al., 1999). This event marked the initial development of an internal sequence of large lagoons, including Araruama (Fig. 1), as well as the formation of the first sand barrier with restinga vegetation. LBE (coordinates 22°56′15" S, 42°14 W -Fig. 1) was formed during the last sea level transgression, between 5.1 and 3.9 kyr. BP, resulting in erosion on the outside sand barrier (Castro et al., 2014; Areias et al., 2020; Araujo et al., 2021).

The LBE is a small (~1 km^2), shallow (<1 m deep), and unpolluted hypersaline coastal lake located 108 km east of Rio de Janeiro city. Water column hydrography is highly variable throughout the year, varying from a few centimeters up to a maximum depth of 0.5 m, with salt content ranging from 55 ppm to ~181 ppm, characterizing hypersaline conditions (Barbosa, 1997; Bahniuk et al., 2015).

The region presents a semi-arid climate, with a negative water balance, as evaporation exceeds precipitation due to the influence of the offshore western boundary upwelling system, which is more active

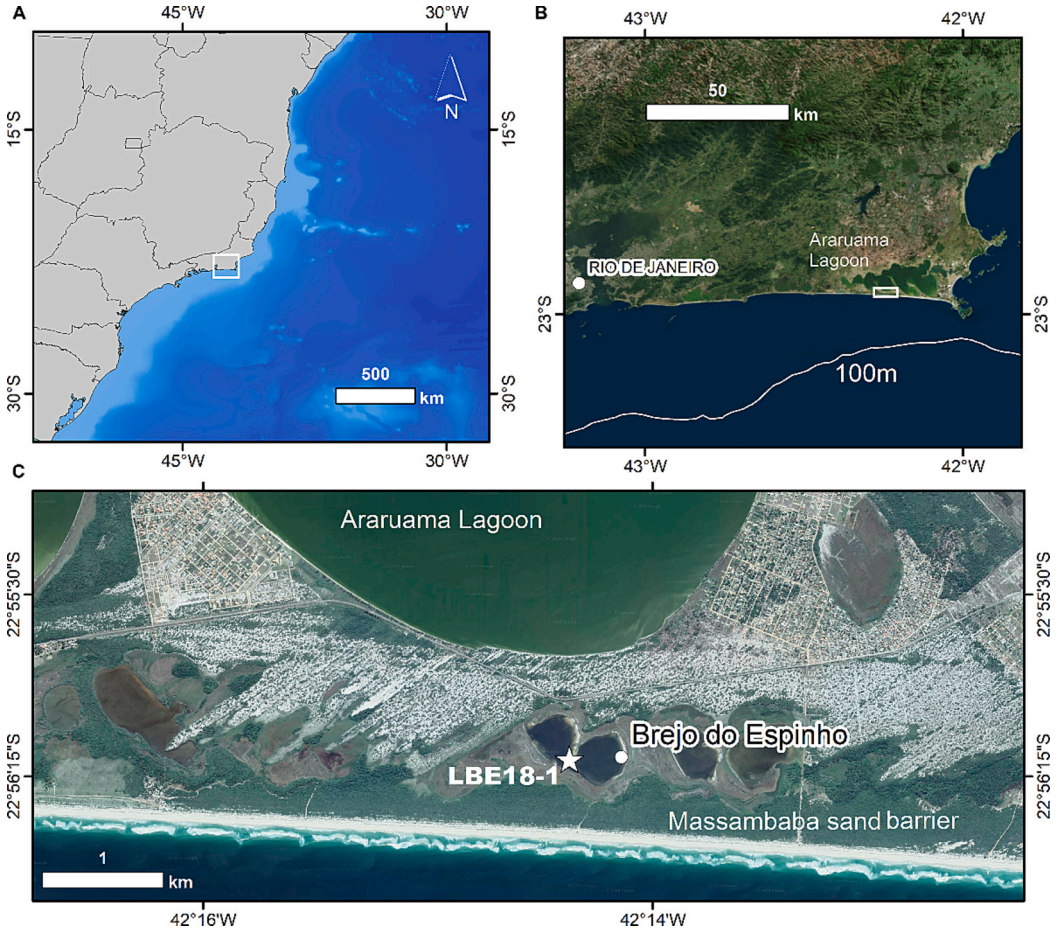

Fig. 1. Brejo do Espinho coastal lake (LBE) located in southern Brazil (A), 108 km east of the Rio de Janeiro city (B). LBE is positioned between the Massambaba sand barrier and Araruama lagoon (C).

during summer and spring (Valentin, 1984; Barbiere and Coe, 1999). The upwelling is facilitated by a narrow coastal shelf with a 100 m isobath close to the coastline and is intensified by strong northeast trade winds that contribute to the upwelling of cold South Atlantic Central Water, promoting an increase in evaporation and dry regional conditions (Moreira da Silva, 1968, 1973).

The regional hydrological balance is mainly distinguished by wet (Austral fall and winter) and dry seasons (Austral spring and summer), when LBE is recharged with meteoric and seawater, respectively (Vasconcelos and McKenzie, 1997; Van Lith et al., 2002). Initially, LBE was connected to Araruama lagoon, resulting in organodetritic sedimentation (Barbosa, 1997). However, this connection was closed at approximately 4 kyr. BP, due to a drop in relative sea level (Castro et al., 2014; Areias et al., 2020), leading to physico-chemical changes and carbonate precipitation (Barbosa, 1997). Seawater is the main dolomite forming fluid that seeps through the Massambaba sandy barrier, into the evaporated hypersaline microbial lake system, primarily during summer (Fig. 1).

The lake's surficial sediments (~ 0–5 cm, Nascimento et al., 2019) are organic carbon rich (~4.5%), implying anoxic burial conditions, but show a decreasing trend in TOC content, where the mineral dolomite predominates (79 and 67 cm depth, Areias et al., 2022), indicating that TOC at these depths is consumed by the bacterial activity (Nascimento et al., 2019; Areias et al., 2022). The first 1 m of LBE sedimentary sequence represents the last ~1.6 cal. kyr. BP (see Areias et al., 2022 for further information about radiocarbon dating and age model). LBE sediments are composed of alternating organic carbon-rich layers and Mg-carbonate-rich layers, including low Mg-calcite (0–4 mol% [(Ca, Mg)CO_3]), high-Mg calcite (>4 mol% [(Ca, Mg)CO_3]), Ca-dolomite (30 to 45 mol% [Ca, Mg$(CO_3)_2$]), and stoichiometric dolomite (30 to 45 mol % [CaMg$(CO_3)_2$]), which precipitate authigenically in the evaporative lake (Tucker, 1988; Vasconcelos and McKenzie, 1997).

Thick microbial mats (~ 0–5 cm) cover the surface of the lake during the dry season (Fig. 2 A-C, Bahniuk et al., 2015). In its multilayered structure (Fig. 2B), photosynthetic activity by cyanobacteria increases oxygen concentration at the uppermost sediment layers in the microbial mat (0–2 mm). This oxygen is rapidly consumed by aerobic respiration and/or sulfide oxidation within the deeper layers (Vasconcelos et al., 2006; Laut et al., 2017, 2019; Fichtner et al., 2023). Throughout its extension, low Mg-calcite precipitation is related to aerobic respiration in the upper sections of the mats, while dolomite and other high Mg-carbonate minerals precipitate at the underlying anoxic layers under sulfate reduction carried by the microbial communities (specifically *Desulfovibrio*), through a process referred to as microbially-induced carbonate precipitation (Vasconcelos and McKenzie, 1997; Van Lith et al., 2003; Vasconcelos et al., 2006). With further burial and early diagenetic processes, high-Mg calcite and Ca-dolomite are converted to stoichiometric dolomite (Vasconcelos and McKenzie, 1997). The microbial mats also support proto-stromatolite formation (Fig. 2D) (Spadafora et al., 2010) Other parameters such as high temperature, salinity, and seawater input have also been suggested to play a major to the microbial induced carbonate precipitation process (Bahniuk et al., 2015; Moreira et al., 2004; Van Lith et al., 2002).

3. Methods

3.1. Sediment sampling

A 100 cm long sediment core (LBE18–1) was retrieved in June of 2018 at the center of LBE using a 10 cm diameter PVC tube (Fig. 1, white star). The core was split lengthwise into two halves and lithologies were described. It was sampled at 2 cm resolution and stored in zip lock bags at +4 °C. Five cubic centimeters of sediment sub-samples for each interval were extracted with a syringe and washed over a 63 μm mesh sieve, to remove fine sediments for foraminiferal analysis. After this procedure, the samples were dried at 50 °C for 24 h and stored dry.

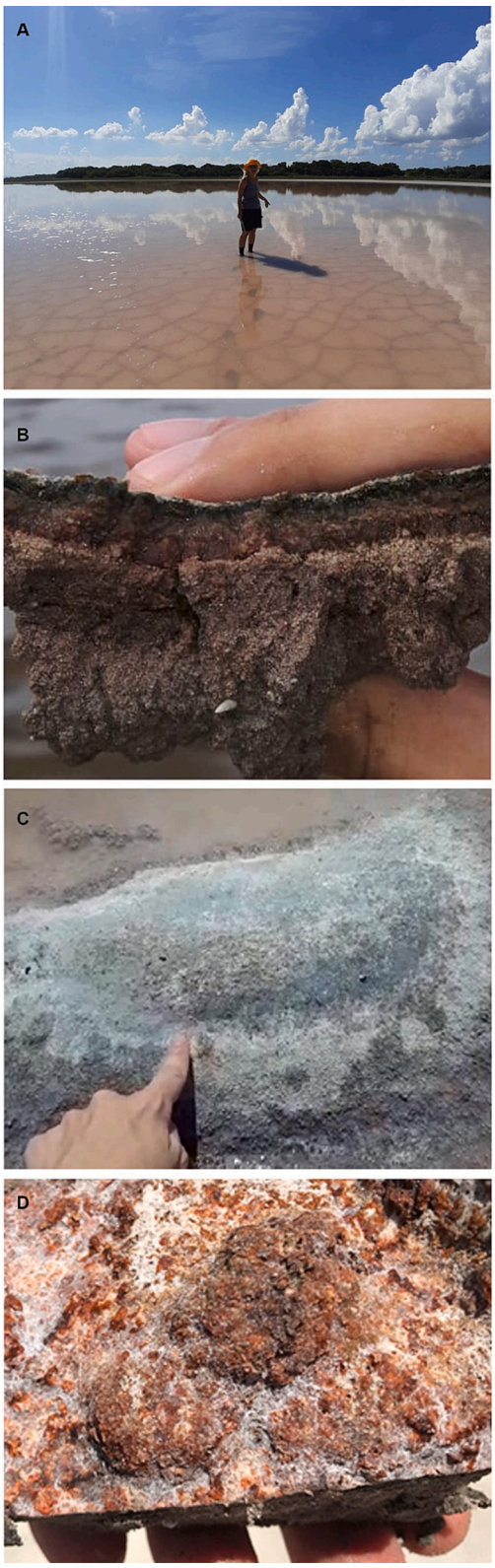

Fig. 2. (A) microbial mat bottom showing the inundated mud crack sediment structure of LBE during the dry season; (B) cross section of the microbial mat showing the sulfate reduction layers at the surface; (C) Bubbles formed by trapped gases below the microbial mat EPS that form an insulating surface like-rubber; (D) Small oranges "proto-stromatolites" are observed, which do not grow beyond the shown size, as they do in neighboring Lagoa Vermelha.

3.2. Laboratory Analysis

3.2.1. Taxonomic identification and pore analysis in Ammonia

Ammonia individuals were picked from selected intervals under a Zeiss STEMI 2000 stereomicroscope. The specimens used were sieved on a 125 μm mesh size to ensure that all individuals were in a similar ontogenetic stage. The specimens underwent a cleaning treatment prior to taking photomicrographs using a Hitachi tabletop Scanning Electron Microscope (SEM)-TM 3000. Briefly, the selected individuals were ultrasonicated inside 1 ml Eppendorf tubes filled with 0.33% H_2O_2 solution. After 30 min, the foraminiferal tests in the tubes were washed three times with 1.5 ml distilled water and dried at 50 °C for 24 h. All individuals were placed on a stub and observed under the SEM.

For pore analysis, the following test parameters were measured according to the semi-automated method described in detail by Petersen et al. (2016).

Analyzed variables include the number of pores (i.e., the total number of pores (Np), pore density (i.e., number of pores per surface area of measurement frame (Np/μm^2)), pore area (i.e., mean surface area of all pores, calculated as the total surface area occupied by pores, divided by the corrected number of pores, expressed in μm^2), and porosity (i.e., percentage of the surface in the measurement frame covered by pores (%).

In the genus *Ammonia*, pseudocryptic (i.e., differentiation based on tenuous or slightly morphological differences), as well as cryptic species (i.e., no morphological differentiation between two species) are observed (Hayward et al., 2004, 2021; Richirt et al., 2019a).

Given the numerous phylotypes in the literature and the high pore variability between them, it's crucial to conduct paleo-O_2 analysis within a single form to avoid bias. For identification, the morphometric parameters measured were average pore diameter, suture's condition (i.e., raised, depressed or flush), the maximum diameter of the specimen (MDS), ornamentation, and porosity following the descriptions of Hayward et al. (2004) and Richirt et al. (2019a). The MDS was measured as the maximal diameter of the entire test of the specimens analyzed using the SEM images with a magnification of 500×, while the average pore diameter was based on the average pore diameter from the average surface covered with pores following the equation:

Surface = (pi)radius^2.

3.2.2. Foraminiferal assemblage analysis

Samples with high individual density were split to obtain a minimum of ~150 specimens per sample, stored on micropaleontological slides for identification. In some sedimentary facies, 150 specimens were not found, while others were barren, but were considered in the paleoecological analysis of LBE because in such an environment their absence indicates extreme conditions. Foraminiferal taxonomic classification was based on the specialized bibliography of Loeblich and Tappan (1988), and Hottinger et al. (1993). For precise identification, all species were imaged using SEM. This ensured accurate identification of the porcelaneous fauna, which are extremely similar. The species were classified as dominant (over 20%), common (10 to 20%), accessory (5 to 10%), and rare or accidental (1–5%), following the definitions of Fatela and Taborda (2002).

For evaluation of community dynamics, cluster analysis of the group average was performed with a second permutation procedure, the similarity profile (SIMPROF) routine to test the presence of sample groups in a priori unstructured sets of samples (Clarke et al., 2008).

The SIMPROF is the set of all resemblances between the specified samples, ranked from smallest to largest (Barbosa et al., 2009). Data were pre-treated by applying a square root transformation, and by calculating the resemblance measure of the Bray Curtis analysis, considering taxa with a relative contribution of at least 5% in any interval of the foraminiferal density data matrix (see Suppl. material). The similarity matrix was also used to perform a Non-metric Multi-Dimensional Scaling (nMDS) ordination to represent the dissimilarity between samples in a low-dimensional space, helping data interpretation. The similarity percentage analysis (SIMPER), was also done to define which species contributed significantly to form the groups at the cluster analysis. All multivariate analysis was performed in Primer v6 software (Clarke and Gorley, 2006).

The community indexes of the Shannon-Weiner Diversity Index (H′), Fisher α index, and the Pielou's evenness (J′) were also measured. These indices were calculated as follows: Shannon-Weiner Diversity Index with the eq. $H' = -\Sigma(Pi*\ln(Pi))$, where Pi is the proportion of individuals per species and ln is the neperian logarithm; Fisher α index: $S = \alpha * ln(1 + n/\alpha)$, where S is the number of species (or species richness), *n* is the total number of individuals, and α is Fisher's alpha; Pielou's evenness with the eq. $J' = H'/\ln(S)$, where H′ is the Shannon-Weiner Diversity Index and ln(S) ln is the neperian logarithm of species richness.

3.2.3. Statistical analysis

The correlation of pore parameters with ancillary data from Areias et al., 2022, was performed using Spearman's rank correlation coefficient on a data matrix (Suppl. material, Fig. 4), with a significance threshold of $p < 0.01$. The data included stable oxygen ($\delta^{18}O$) and carbon ($\delta^{13}C$) isotopic composition of carbonate sediments, TOC, mineralogical fractions (Dolomite and high Mg calcite), and key foraminiferal species.

To verify a possible ontogenetic influence in pore measurements, the pore parameters were plotted against the MDS of *Ammonia* tests, which can be considered as an approximation of ontogenetic stages. Determination coefficients (r) and *p*-values were used to explore ontogenetic effects. All analysis was carried out using R software (R Core Team, 2020, version 4.0.2).

4. Results

4.1. Oxygen proxies

Foraminiferal pore morphometric analysis was applied to 28 of the 50 intervals in triplicate in a total of 84 individuals, since in 22 intervals *Ammonia* tests were not found or did not reach the minimum of 3 specimens required (between 94 and 48 cm depth).

The average porosity and pore area values for each interval covaried within the core. A decrease from the base to the top of the core is observed, ranging from 13% to 27.5% and from 1.9 μm^2 to 6.3 μm^2 (avg. 21% and 3.7 μm^2), respectively (Fig. 3). Pore density and number of pores values range from 0.03 Np/μm^2 to 0.1 Np/μm^2, and from 38 Np to 119 Np, respectively (avg. 0.06 Np/μm^2 and 67 Np). The density and number of pores covaried presenting an inverse pattern to pore area and porosity (Fig. 3). Bulk and average values measured from each interval (cm) are available in Suppl. material.

The MDS and pore diameter varied from 226 μm to 433 μm and from 1.54 μm to 2.82 μm, respectively (avg. 325 μm and 2.1 μm). The MDS covaried with the pore area and porosity values. The MDS varied between 446 μm and 226 μm, with an average value of 331 μm. Pore patterns showed no significant correlation with MDS (Suppl. material), with low determination of coefficients r, as follows: Porosity: ($r = 0.01173$, $p = 0.1626$), area of pores: ($r = 0.05979$, $p = 0.0142$), number of pores ($r = -0.004294$, $p = 0.4242$) and pore density: ($r = 0.02032$, $p = 0.1028$). Thus, we can assume that surface pore variability presents low, or no influence by ontogenetic factors.

Ammonia morphometric parameters presented significant correlations with geochemical data such as TOC, $\delta^{18}O$, $\delta^{13}C$, and mineralogy (Fig. 4). Among the variables, pore area had the highest correlation.

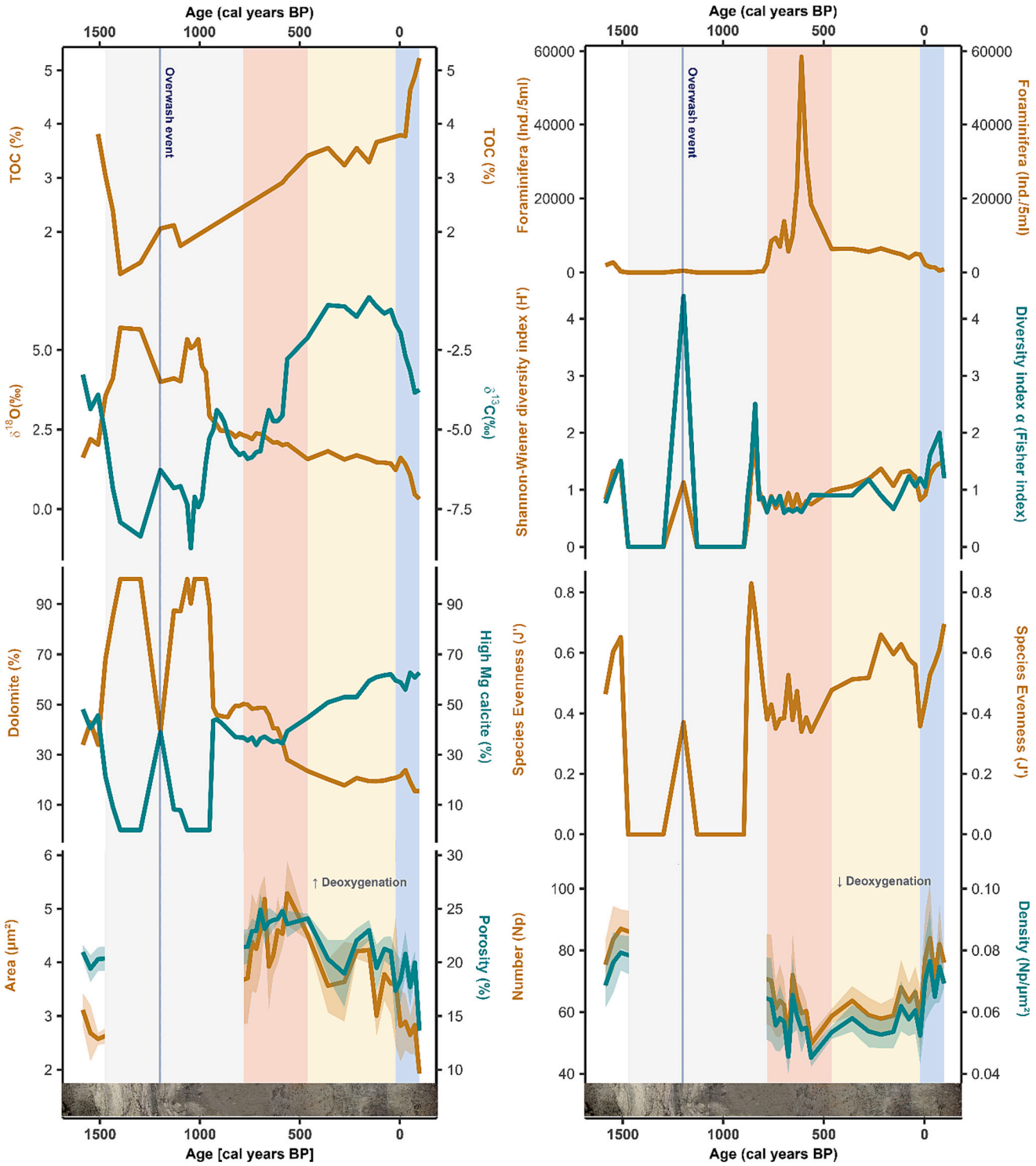

Fig. 3. LBE 18–1 core secondary data plotted against radiocarbon age, Left column: TOC (%), $\delta^{13}C$ (‰), $\delta^{18}O$ (‰), dolomite percentages from Areias et al. (2022), porosity (%) and pore area (µm^2) of *Ammonia* T1. Right column: Foraminiferal density, diversity indices, species evenness and pore density (Np/µm^2) and Number (Np) of *Ammonia* T1. Shaded areas represent max. and min. Values, and thin lines represent the median values obtained from each pore parameter. Colors represent recognized phase 1 (1584–781 cal yrs. BP, white), phase 2 (781–562 cal yrs. BP, red), phase 3 (562–20 cal yrs. BP, yellow) and phase 4 (deposition since 1950, blue) discussed in section 5. (For interpretation of the references to color in this figure legend, the reader is referred to the web version of this article.)

Specifically, pore area correlated negatively to TOC content ($r = -0.84$), indicating that *Ammonia* pores, and hence oxygen availability in the lake are directly controlled by OM degradation with O_2 levels decreasing towards intervals of lower (e.g. residual) OM content in the LBE sedimentological record. Concerning mineral deposition, an intermediate but higher significant correlation to high-Mg carbonates was observed (pore area-dolomite, $r = 0.48$, porosity-dolomite, $r = 0.55$), indicating that increasing dolomite precipitation correlates with increasing levels of deoxygenation in the lake.

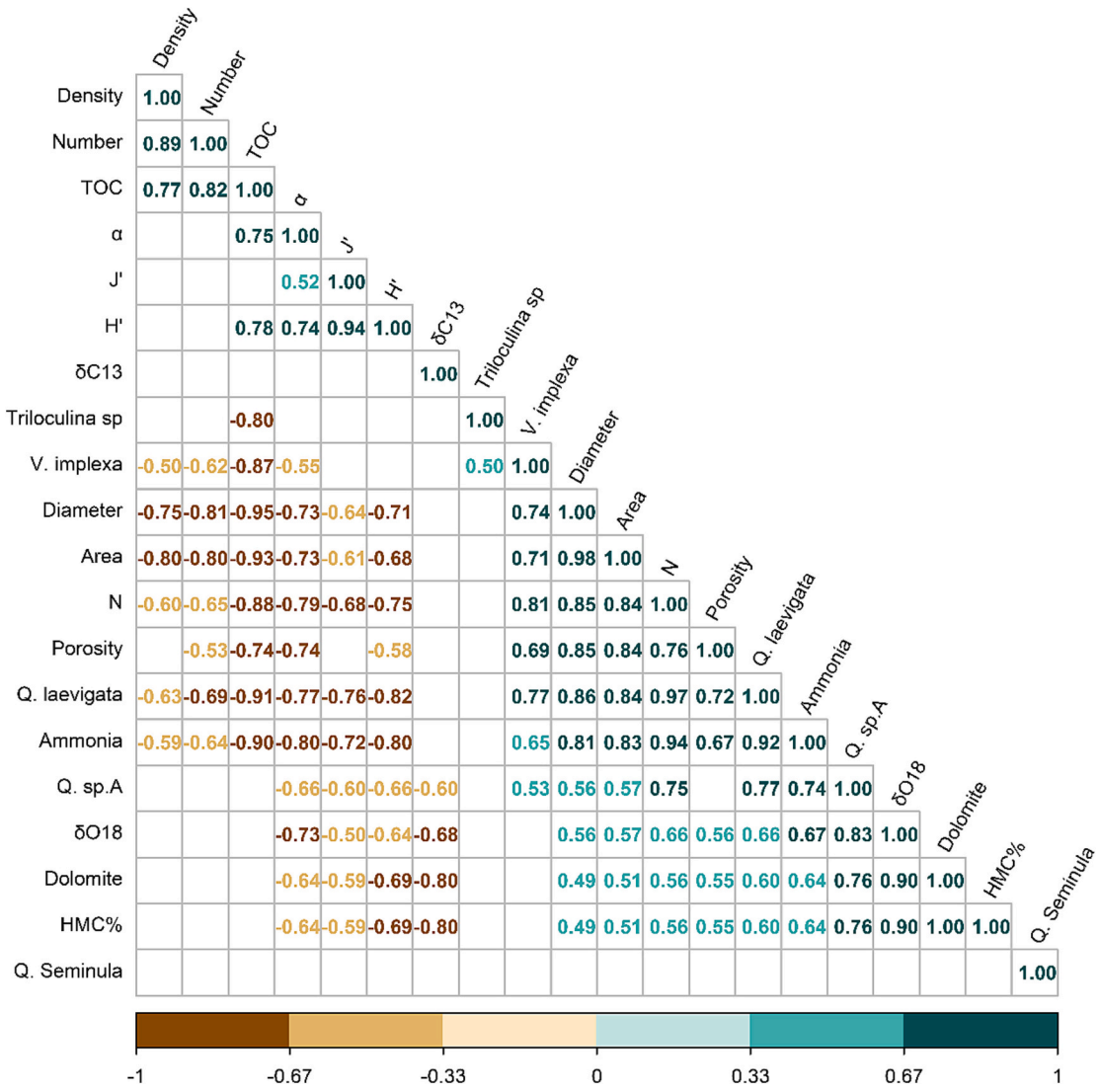

Fig. 4. Correlation map of carbonate mineralogy of the sediment with the Ammonia's pore patterns, geochemical proxies (and sediment grain size %), faunal patterns and key benthic foraminiferal species. The bar on the right indicates the color legend of the Spearman's rank correlation coefficient (*r*) calculated for each couple of parameters in the matrix. A two-sided *p*-value <0.01 was taken to indicate significance for all statistical analyses). Squares in blank denote correlations with no significance. Abbreviations: D% = Dolomite; HMC% = High-Mg calcite; Q. sp.A = Quinqueloculina sp.A; Ammonia = *Ammonia* cf. *A. veneta* (Schultze, 1854) see in Hayward et al. (2023).

4.2. Foraminiferal community and taxonomical indices

A total of 26 species were found in the core (Figs. 5 and 6), comprising 8 families (i.e *Ammoniidae, Elphidiellidae, Trichohyalidae, Haueriniae, Rosalinidae, Fischerinidae, Bolivinitidae, Buliminidae, Cassidulinidae, Globigerinidae, Gavelinellidae, Planulinidae, Uvigerinidae*), from the orders Miliolida and Rotaliida.

The species *Q. laevigata*, and *Triloculina* sp. were considered dominant (> 20%) in some intervals with an average relative abundance of 67.9% and 12.8%, respectively. *Ammonia* cf. *A. veneta*, *Miliolinella* sp., *Quinqueloculina* sp.2, and *Varidentella implexa* were determined to be accessories (5 to 10%). *Trifarina bradyi*, *Planulina foveolata*, *Rosalina globularis*, *Bolivina aenariensis multicostata*, *Bulimina marginata*, *Cassidulina curvata*, *Gyroidina umbonata*, *Globigerinoides ruber*, *Pyrgo* sp., and *Wiesnerella auriculata* were considered rare (>5%), but responsible for a taxonomic composition shift in foraminiferal assemblages from the intervals 85 cm and 55 cm.

For *Ammonia* identification (Fig. 6, individual 37 A-C), measured size of the specimen's test (331 ± 44 μm, present study) agrees with the size measurement values of 220–400 μm for T1 phylotype calculated by Hayward et al. (2004) and just slightly higher than the 265 ± 44 μm described by Richirt et al. (2019a). The measured pore diameter (2.1 ± 0.34 μm, present study) is also compatible with that by Richirt et al. (2019a) of 1.96 ± 0.34 μm for T1. The specimens found also presented raised sutures as described for T1 species in the ventral side, but with maximum porosity values of 27.5%, which slightly surpassed the average upper limit of 25% defined for T1 species (Richirt et al., 2019a). Considering the morphometric definitions of Hayward et al. (2004, 2021) and Richirt et al. (2019a), we associate LBE 's individuals of *Ammonia* as corresponding to a single phylotype (T1) throughout the entire core (Fig. 5).

To further evaluate this, a comparison of morphological identifications using pore diameter data and suture conditions was performed between LBE populations and the other 137 individuals of *Ammonia* that were also subjected to molecular analysis (Saad and Wade, 2016; Richirt et al., 2021) (see Suppl. material). As in the above mentioned data, the

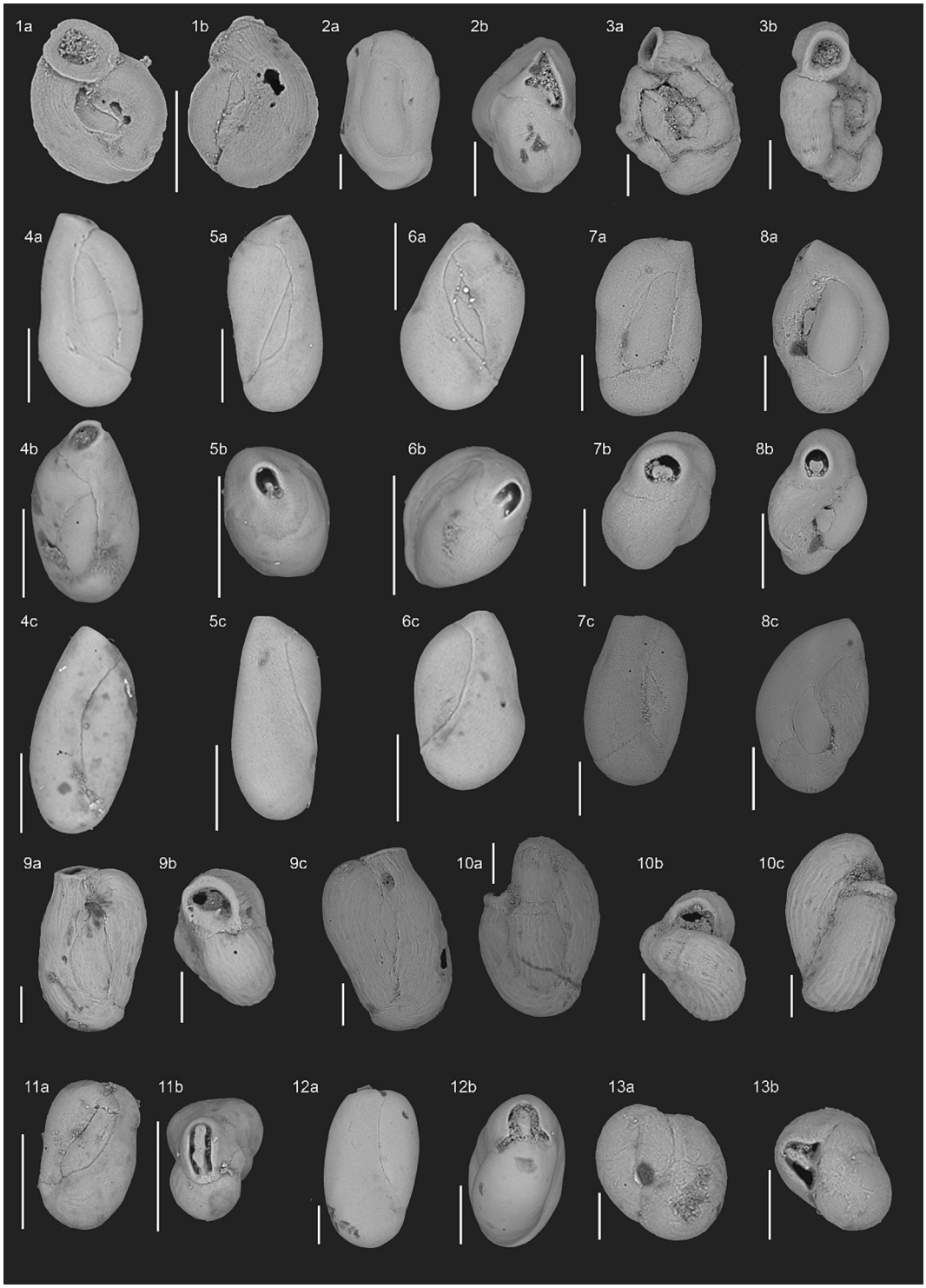

Fig. 5. 1a, b *Wiesnerella auriculata*: side views. 2a, b *Lachlanella* sp.: side views. 3a, b *Massilina protea*: side views. 4,5,6 Ecophenotypic forms of *Quinqueloculina laevigata*: 4a,5a,6a, side views; 4b,5b,6c, apertural views, 4c,5c,6c, side views. 7,8 Ecophenotypic forms of *Quinqueloculina seminulum*: 7a,8a, side views; 7b,8b, apertural views, 7c,8c, side views. 9,10 *Quinqueloculina* sp.A: 9a,10a, side views, 9b,10b, side views. 11, 13 *Affinetrina* sp.: 11a,13a, side views, 11b,13b, apertural views. Each number represents a different individual. Scale bars represent 100 um.

analysis supports the assignment, showing that specimens from LBE exhibit raised sutures and pore diameters (2.1 ± 0.34 μm) within the same range as T1 specimens (2 ± 0.44 μm, Suppl. material). However, a genetic analysis is further necessary to validate this morphological assignment.

Following the recent taxonomic assignments by Hayward et al. (2021) for *Ammonia* phylotypes, all specimens found at LBE would correspond to *Ammonia veneta*. However, due to the limitations of a morphological approach, our specimens are hereafter assigned as *Ammonia* cf. *A. veneta*. We note, however, that this assignment has rarely been used along the Brazilian coast (Sariaslan and Langer, 2021), not matching with the historical use of *Ammonia tepida* in LBE (Barbosa, 1997) and nearby settings (Debenay et al., 2001; Raposo et al., 2018; Belart et al., 2019; Laut et al., 2022).

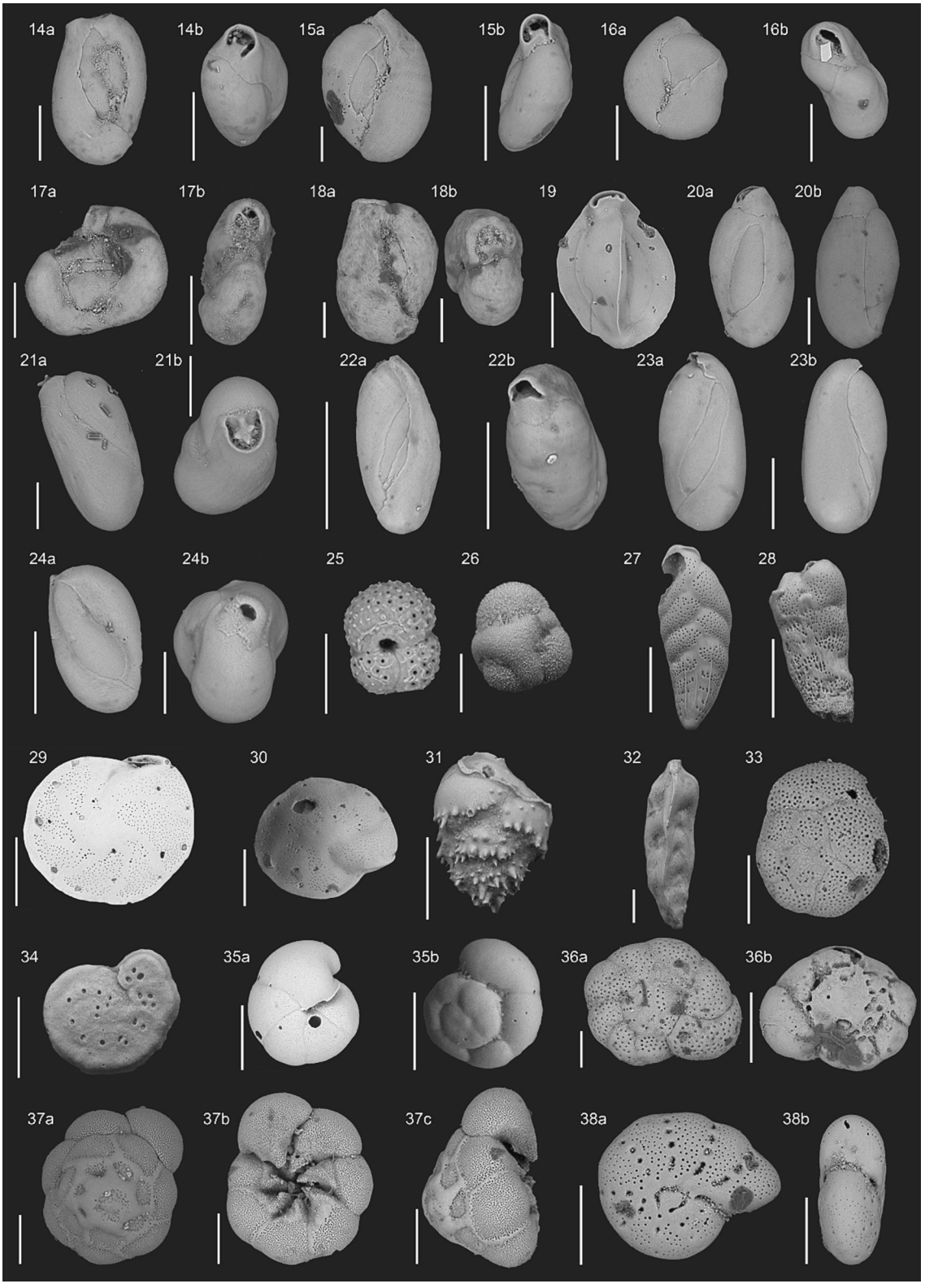

Fig. 6. 14,15,16 *Miliolinella* sp.: 14a,15a,16a, side views, 14b,15b,16b, apertural views. 17 *Neopateoris* sp.: 17a, side view, 17b, apertural view. 18 *Pseudotriloculina subgranulata:* 18a, side view, 18b, apertural view. 19 *Pyrgo* sp.: side view. 20 *Triloculina* sp.: 20a, b side views. 21 *Triloculina lutea*: 21a, side view, 21b, apertural view. 22,23,24 *Varidentella implexa*: 22a,23a,b, 24a side view, 22b,23a,24b apertural views. 25,26 *Globigerinoides ruber*: ventral views of individuals without and with bula, respectively. 27, 28 *Bolivina aenariensis multicostata:* Side views. 29,30 *Cassidulina curvata:* spiral views. 31 *Bulimina marginata:* Side view. 32 *Trifarina bradyi*, side view. 33 *Rosalina globularis:* spiral view. 34 *Planulina foveolata*: spiral view. 35 *Gyroidina umbonata*: 35a, ventral view, 35b, dorsal view. 36 *Trichoyalus* aquayoi: 36a, spiral view, 36b, umbilical view. 37 *Ammonia veneta*: 37a, spiral view, 37b, umbilical view, 37c side view. 38, *Elphidiella* sp.: 38a, side view, 38b, peripheral and apertural view. Each number represents a different individual. Scale bars represent 100 um.

The micropaleontological record of the LBE core has several low diversity indices, such as Fisher α index (av. 1.1), Shannon-Weiner Diversity Index (av. 1), and Richness (av. 21) (Suppl. material). The correlation with secondary geochemical data shows that biotic parameters (Fisher α index, Pielou's evenness, and Shannon-Weiner Diversity Index) correlate negatively with increasing dolomite formation and relative decrease of oxygenation (Fig. 4).

With a 5% cut-off, only the species *Ammonia* cf. *A. veneta*, *Miliolinella* sp., *Quinqueloculina* sp.2, *Q. seminulum*, *Q. laevigata*, *Triloculina* sp., *T. lutea*, and *V. implexa* were considered for the faunal assemblage data. Hierarchical clustering based on Bray-Curtis similarities distinguished five major interval groups, which mainly presented a temporal distribution in the core, as follows: facies "b" (95,85, 57 to 55, and 3 cm depth), facies "e" (47 to 37 cm depth), facies "c" (35 to 29 cm depth), facies "f" (27 to 11 cm depth) and facies "d" (99, 97, 49, 9 to 1 cm depth). Facies "a", which consists only of the 59 cm depth interval, presented no similarity to any other interval. Bulk data of the main species for each group, biotic census, ^{14}C data, and nMDS plot of foraminifera abundance can be found as Supplementary data.

5. Discussion

The effect of oxygen oscillations on the pores of foraminifera tests has been demonstrated in recent studies (Petersen et al., 2016 and references herein) and these variations can be observed in long-term records. The development of tools for diagnosing the fluctuation of this gas is crucial, as the concentration in marine ecosystems has already declined by 2% since the 1960s due to global warming, a trend that is expected to continue (Long et al., 2016).

The search for the effects of hypoxia in shallow coastal areas through foraminiferal tests uses pore size analysis on hyaline tests of foraminifera because porcelaneous have no pores and agglutinant communities are accessory and considered to be hypoxic-sensitive (Levin et al., 2009). However, due to the natural extreme conditions, LBE microbial mat (Fig. 2) is dominated by porcelaneous species, with no agglutinant and only a few hyaline taxa are found, representing a key environment to the study of the specific responses of foraminifera in high evaporative coast. In addition, the low hydrodynamics, and high alkalinity favors preservation of subfossil assemblages in modern conditions. In the studied core, most specimens were pristine, despite some deformities, which are common in hypersaline settings (Barbosa, 1997; Debenay et al., 2001; Geslin et al., 2002), with low taphonomic distortion, important for reliable palaeoecological and pore morphometric analysis.

In general, the lake presents relatively low diversity values (average Fisher α index of 1.1, Shannon-Weiner Diversity Index values of 1), with major species belonging to only one family, *Hauerinae*, with commonly found taxa also seen in other nearby settings, e.g., *Ammonia*, *Elphidium*, *Quinqueloculina*, *Triloculina*, *Lachlanella*, and *Miliolinella* (Barbosa, 1997; Debenay et al., 2001; Geslin et al., 2002; Raposo et al., 2018; Belart et al., 2019; Laut et al., 2022). On the other hand, foraminiferal density varied significantly from 0 to 58,560 ind./5 ml.

Concerning the morphometric analysis, test pores followed the same trends observed by Richirt et al. (2019b), in which the density and number of pores followed a negative correlation with an increase of porosity and surface area (Fig. 4). These authors postulate that pore size increases to enhance the gas exchange as a response to the reduction of dissolved oxygen in the water, thus, a decrease in density and number of pores occurs to preserve the mechanical constraints of the tests. The pore area presented a negative correlation with TOC content ($r = -0.84$), revealing that *Ammonia* pores are directly controlled by the degradation of OM in the LBE sedimentological record increasing towards intervals of lower oxygen content. This assumes that TOC levels were similar upon deposition and the low TOC is a result of respiration and corroborates with previous data of higher pore area in hyaline tests in such conditions (Petersen et al., 2016; Rathburn et al., 2018; Lu et al., 2021). This is evidenced as porosity patterns keep up with the negative trend of $\delta^{13}C$ (Fig. 3), indicating incorporation of ^{12}C-depleted dissolved inorganic carbon, released by the sulfate-reducing and other heterotrophic bacteria during intense decomposition of organic matter (Vasconcelos and McKenzie, 1997; Sánchez-Román et al., 2009; Nascimento et al., 2019; Fichtner et al., 2023), and higher dolomite precipitation. The intense microbial activity consumes O_2 during bacterial respiration, driving the correlation of porosity patterns with the negative trend of $\delta^{13}C$ values (see Fig. 3).

LBE18–1 core dating (Areias et al., 2022) shows that the samples represent the last ~1.6 kyr, which only comprises the lacustrine facies of the lake, established since its isolation from the ocean, which occurred at around 3600 B.P. (Barbosa, 1997; Castro et al., 2014; Araujo et al., 2021). In this context, pore metrics and community dynamics presented here are not related to sea-level changes, once this is lowering since the last transgressive maximum that occurred at 5.0 ka, but respond predominantly to lacustrine processes dominated by evapo-precipitation and tide influence through the Massambaba sand barrier, with overwash event easily detected due to suddenly occurrence in the register of high diversity shelf species.

The combination of redox proxies and the foraminiferal community structure resulted in four distinct phases (Table 1), identified as follows: phase 1 (1584–781 cal yrs. BP), phase 2 (781–562 cal yrs. BP), phase 3 (562–20 cal yrs. BP) and phase 4 (modern samples deposited after 1950).

5.1. Phase 1

The first phase (1584–781 cal yrs. BP, Fig. 3) is marked by (mostly) barren facies (phase 1a) and apparent recovery of foraminiferal faunas from a stressful event (phase 1b). Considering the local geochemical data from these same intervals, extreme arid conditions are recognized by Areias et al. (2022) between 1500 and 1000, which matches stratigraphically with the highest percentages of dolomite in the core and the complete elimination of the foraminiferal community (Fig. 3, Table 1). In these intervals, $\delta^{13}C$ is depleted, shifting to −8.7 ‰ at 1044 cal yrs. BP, which indicates an increase in bacterial activity, in this case, anaerobic sulfate reduction that consumes lacustrine organic matter and oxygen (Fig. 3). The enrichment of $\delta^{18}O$ at the core bottom means high evaporation around 1000 BP, in a significant dry phase with higher dolomite precipitation in LBE (as noted by Vasconcelos and McKenzie, 1997; Nascimento et al., 2019; Areias et al., 2022). This explains why no foraminifera was found over 575 years between the intervals 93 cm (1471 cal yrs. BP) and 61 cm (896 cal yrs. BP), abruptly responding to the changes in the local environment, recorded in the geochemical

Table 1
Summary of ecological, pore area, XRD, and geochemical data according to different carbonate depositional phases of LBE-18 core.

Phase	SIMPER	Density (ind./5 ml)	H′	J′	S	Pore area (μm²)	TOC (%)*	Dolomite (%)*	$\delta^{13}C$ (‰)*	$\delta^{18}O$ (‰)*	Age (cal yrs BP)*
1a	Mostly barren	30	0.15	0.06	1.2	ND	2	81.57	−6.54	4.22	1584–896
1b	Facies b, d	517	0.88	0.54	5.3	ND	ND	47.84	−5.44	2.38	896–781
2	Facies e, c	18,505	0.78	0.39	7.2	4.5	2.97	43.44	−4.93	2.19	781–562
3	Facies f	5470	1.16	0.53	8.6	3.8	3.45	20.23	−1.34	1.53	462–20
4	Facies d	1281	1.18	0.49	10	2.6	4.46	19.14	−3.08	0.97	After 1950 CE

* Data from Areias et al., 2022

proxies. Since foraminiferal communities only start to reoccur at 896 cal yrs. BP, we propose that aridity must have been more prolonged than described by Areias et al., 2022. This pattern has also been recognized by Barbosa (1997), who studied the local foraminiferal assemblages in LBE, showing a strong decrease in absolute abundances of foraminifera at the same age intervals.

Between 1471 and 896 cal yrs. BP sediments (phase 1a), foraminifera were only found at 86-84 cm depth (around 1196 cal yrs. BP), which comprised the interval of greatest richness in LBE with the occurrence of 21 species. The interval presents a community that is composed of 13 species derived from in situ populations as well as 8 rare species that are commonly found in the continental shelf of the Campos Basin (Vieira et al., 2015), which only occurred in this interval. These include: *Trifarina bradyi, Planulina foveolata, Bolivina aenariensis multicostata, Bulimina marginata, Cassidulina curvata, Gyroidina umbonata, Rosalina globularis*, and the planktonic *Globigerinoides ruber*. This Foraminifera occurrence matches stratigraphically with an abrupt change in the sedimentary geochemistry of LBE with reduced dolomite percentages, more positive $\delta^{13}C$ values, and lower porosity patterns in *Ammonia* cf. *A. veneta* (i.e., higher oxygenation). Considering LBE faunal pattern, the increase in the species richness at 86-84 cm indicates the occurrence of an oceanic overwash during the high dolomite forming period, which transported open water species into the lake system. This could have happened during a strong storm, for example, when the Massambaba sand barrier (Fig. 1) wasn't as long or as tall as it is today.

This is evidenced by the fact that the specimens are mostly broken, small, corroded and represented by only a few individuals. At 56-54 cm, 840 cal yrs. BP, a few taxa of rare occurrence as *Globigerinoides ruber, Pyrgo* sp., and *Wiesnerella auriculata* are also found, indicating a similar shift to seawater, as seen in the geochemical markers at 86-84 cm (1196 cal yrs. BP). At this interval, Areias et al. (2022) identified a high C/N ratio (around 14), which corroborates the influence of mixed organic matter, whereas land-plants derived OM could have been transported to the area by wind action or runoff. Foraminifera size and preservation of marine species document that overwash events happened and influenced biotic and geochemical shifts at LBE, including dolomite formation by delivering the necessary ions to calcium magnesium carbonate precipitation.

By the end of phase 1a, from 877 to 801 cal yrs. BP (60 to 50 cm depth, phase 1b) the foraminiferal fauna begins to gradually recover. This phase is marked by assemblages of relatively low abundances (avg. values of 264 ind/5 ml), defined in cluster b, in which *Q. laevigata* and *Triloculina* sp., are the most representative taxa (43% and 23%, respectively). The species *Q. laevigata* is the first to reoccur in the lake, followed by *Miliolionella* sp., and *Quinqueloculina* sp. 2, while *Ammonia* is the last genus to appear at 48-46 cm (760 cal yrs. BP), indicating a relatively lower tolerance than miliolids.

5.2. Phase 2

Phase 2 between 760 and 562 cal yrs. BP (average intervals of 48 to 28 cm depth) comprises the intervals of greater porosity and pore area in foraminiferal tests of *Ammonia*, indicating low oxygenation. This shows the prevalence of sulphate reducing over oxygenic conditions (i.e., sulfate reducers and/or aerobic heterotrophic bacteria over photosynthetic cyanobacteria) at surficial sediments (0–6 mm). Foraminiferal density appears not to be negatively influenced by low oxygen conditions, with higher densities occurring in the highest porosity intervals. Such a significant positive correlation between oxygen and pore area is true for both *Ammonia* ($r = 0.82$) and the most prominent taxa in the core, *Q. laevigata* ($r = 0.83$), both which present dense populations over these intervals. This suggests an opportunistic behavior to increase low oxygen tolerance under extreme conditions. Other species such as *V. implexa*, and *Quinqueloculina* sp. 2 also show an increase of their relative abundance. However, any foraminiferal density is relatively lower than those of *Q. laevigata* which reaches over 85% of average relative contribution leading to high dominance to all these intervals.

Among all, *Ammonia* is a well-studied genus, with their biological thresholds regarding temperature (Bradshaw, 1957), and oxygen (Bernhard and Sen Gupta, 1999; Nardelli et al., 2014; LeKieffre et al., 2017) well described. *Ammonia* presents a widespread distribution and previous studies have also documented the increase in their populations towards oxygen depletion areas (Ye et al., 2012; Richirt et al., 2020, 2022), confirming the trend of increased porosity in the individuals analyzed here. In addition, the genus is known to be resistant to anoxia and, as previously discussed, are commonly found with dense populations in anoxic settings. The high statistical correlation in our study indicates that *A. veneta* occurrence itself and the surface test morphometric parameters analyzed are both good indicators for O_2-variability. However, phase 2 probably presented severely oxygen-depleted conditions but not complete anoxia. *Ammonia* can survive and calcify under hypoxic conditions (Bernhard and Sen Gupta, 1999; Nardelli et al., 2014), but under prolonged severe anoxia, *Ammonia* exhibits perturbation of normal physiological processes, and it can even consume its cytosol (LeKieffre et al., 2017; Koho et al., 2018).

Notably, the most prominent taxa of LBE, *Quinqueloculina* cf. *Q. laevigata*, haven't been linked to anoxia in recent literature. However, it does exhibit correlation with the oxygen proxies used here. In fact, many *Quinqueloculina* species are known to be hypoxic sensitive (Wang et al., 2014). Previous reports of *Quinqueloculina* cf. *Q. laevigata* as a dominant species in sediments are also unknown, but it is commonly found in the Mediterranean Sea as an accessory species in shallow water environments <15 m deep of lower hydrodynamic energy (Buosi et al., 2012), and in shallow hypersaline environments (Abu-Zied and Bantan, 2013; Amao et al., 2018), often presenting correlation with muddy sediments, TOC, and temperature (Abu-Zied and Bantan, 2013; Al-Dubai et al., 2018; Kaushik et al., 2019). In fact, the miliolids species presented high morphological diversity in the lake, and the miliolids here identified as *Quinqueloculina* cf. *Q laevigata* could be a polytypic variation of the species *Q. seminulum* (see Kaushik et al., 2019), which is also dominant in Lagoa Vermelha, at similar conditions of high TOC and temperature (Barbosa, 1997; Laut et al., 2022). This pattern was also observed by Debenay et al. (2001) for *Triloculina oblonga* in adjacent Araruama lagoon. For observation of the transitional variations between *Q. seminulum* and *Q. laevigata* see Fig. 4 and Fig. 5. Nevertheless, adding to the previous indications (Wang et al., 2014), it is possible to associate some *Quinqueloculina* spp., as tolerant to low O_2-conditions.

Bacterivory is common in foraminifera communities, and they have been recorded to have a substantial effect upon bacterial communities by harvesting biofilm (Bernhard and Bowser, 1992; Laut et al., 2016; Chronopoulou et al., 2019; Schweizer et al., 2022). Jorissen et al. (1998) observed that infaunal foraminiferal densities present close correspondence with the depth distribution of microbial processes of sulfate reduction, which suggests that infaunal foraminifera would feed selectively, either on the bacterial stocks or on nutritious particles produced by bacterial degradation of more refractory organic matter. The bacteria communities are highly abundant in LBE (Delfino et al., 2012), and due to their capacity of producing exopolymeric substances of high nutritional value, they could sustain and favor high-density populations of foraminifera with increased food availability. Similar association between bacterial biomass and foraminifera distribution, richness, and diversity has also been observed in polluted estuarine regions of Brazil (Laut et al., 2016). In general, *Quinqueloculina* spp. display significant tolerance to organic enrichment (O'Malley et al., 2021), indicating presence of high quality organic-rich food sources. The relatively high resistance to extreme conditions coupled with rich food supply could explain the high dominance of *Q. laevigata* and the general increase of other miliolids species at depth with high TOC. However, H_2S is recognized to occur at Brejo do Espinho sediments in modern conditions at low values (0.2 mM in the uppermost 25 cm) and higher microbial activity indicated by $\delta^{13}C$ suggest the prevalence of sulfidic conditions, which is known to be fatal to foraminifera when exposure is long

(Moodley et al., 1998; Moreira et al., 2004). Following the geochemical biomarkers, the increase of H_2S could be an additional factor for the foraminifera barren facies observed during the high dolomite forming phase 1.

5.3. Phase 3

After recovering from the dolomite formation period, foraminiferal absolute abundance and dominance displays a decreasing pattern for most foraminiferal species in phase 3, which accompanies a relative increase of oxygen, indicating an improvement of environmental conditions in the lake between 460 and 20 cal yrs. BP (average intervals of 28 to 10 cm depth, Fig. 3). However, their relative contributions remain constant within more oxidized sediments. A major shift in foraminifera communities occurs only between the relative abundance of *Q. laevigata* and *Triloculina* sp. At around 276 and 215 cal yrs. BP (24 and 20 cm) when *Triloculina* sp. abundance increases, and the species contributes similarly to the assemblage. These intervals presented moist conditions as inferred with the decrease in Ca/Ti, Ca/$\sum$ (Ti, Fe, Al), ln(Ca/Ti) and ln(Br/Ti) (Areias et al., 2022) suggesting higher water level, lower salinity, and less authigenic carbonate formation. In this phase both species are dominant (>20% of relative contribution), but *Triloculina* sp. cannot be regarded as an appropriate indicator of relative improvement in the ecosystem since the species did not present a significant correlation to any geochemical data in LBE.

5.4. Phase 4

In phase 4 that represents recent deposition (after 1950 CE), all faunal patterns (avg. values for J' of 0.6, H′ of 1.2 and α of 1) continue to indicate relative improvement of environmental conditions with facies "d" that presents close correspondence with lower microbial activity and lower evaporation, thus lower dolomite formation, occurring at both surface sediments (After 1950 CE, dolomite >19%) and the base of the core (1584–1508 cal yrs. BP, dolomite >37%), before the establishment of the aridity trend. With the relative improvement, more regular occurrences of *Trichoyalus* aquayoi, *Neopateoris* sp., *Affinetrina sommeri*, and *Affinetrina* sp. were also observed as rare species (1–5%).

In agreement with the ancillary data, a higher variation in *A. veneta* test porosity following a decreasing trend indicates more oxidation towards modern conditions. According to Lu et al., 2021 with such variability the pore area does not necessarily well constrain oxidized conditions. Thus, the high variability must occur due to the increased prevalence of periodic variation of local conditions, possibly in function to the seasonal influence of local dry climate regime and upwelling conditions, similar to what occurs nowadays in LBE. Another possibility is that despite the results of our morphological analysis more phylotypes could be occurring in the lake, which could be confirmed through genetic analysis.

6. Conclusion

Understanding microbe-mineral interactions is crucial for interpreting paleo records and our results have enabled the investigation of O_2-dynamics during different dolomite deposition phases. The present study conducted a quantitative analysis of coupling benthic foraminifera assemblages and surface porosity in *Ammonia* populations, observing their fluctuations during dolomite precipitation. Along different depositional phases, pore area indicated increased deoxygenation at the sediment-water interface marking the prevalence of anaerobic process (e.g., sulphate reduction) over oxygenic conditions during phases of higher microbial activity and dolomitization. The foraminiferal assemblages from LBE are mainly composed of stress-resistant taxa and the taxa *Quinqueloculina* cf. *Q.laevigata* and *Ammonia* turned out to be good bioindicators of O_2-depleted conditions, of which density and dominance correlate with oxygen level proxies, particularly the pore area, and marked aridity intervals.

High dolomite concentration of up to 50% towards the core base resulted in the complete elimination of the foraminifera community, and barren facies indicate that aridity must have endured for at least 575 years between 1471 and 877 cal yrs. BP. During this phase, possible overwash events occurred marked by changes in LBE community structure with the addition of common species found in the Campos Basin continental shelf. The entrance of oceanic waters into the lake is likely to have influenced biotic and geochemical signatures as observed in this study. Overall, the data show that pore analysis in hyaline foraminifera can significantly improve our understanding of redox conditions. It provides morphological signature for the bioindicator species and influences the biodiversity of the community structure of these protists that are at the base of the trophic web. Additionally, the enhancement of this pore analysis tool and increased generation of historical and paleoenvironmental data, in the context of warming and reduced ocean ventilation scenarios, represent a new frontier that is necessary to improve predictions of future changes.

Authorship statement

DF: Investigation, formal analysis, visualization, writing - original draft, editing; CFB: Supervision, conceptualization, data curation, project administration, resources, funding acquisition, writing, editing; CA, ND, LGRSV, APSC, JCSS, CV, NMS, DSS, AP: Methodology, validation, writing and editing.

Declaration of Competing Interest

The authors declare that they have no known competing financial interests or personal relationships that could have appeared to influence the work reported in this paper.

Data availability

Data will be made available on request.

Acknowledgments

CFB acknowledges the Buzas Award for Travel (BAT) received from the Cushman Foundation for Foraminiferal Research. This study was financed in part by the Coordenação de Aperfeiçoamento de Pessoal de Nível Superior - Brasil (CAPES) – Finance Code 001. DF thanks the scholarship of the Rio de Janeiro Research Support Foundation (FAPERJ) Process No. E-26/201.780/2018 and CNPq No. 132210/2020-7. CA thanks to the FAPERJ Nota 10 scholarship and the funding of the Swiss Government Excellence Scholarship. Thanks to Dr. Julien Richirt for help with the Ammonia identification. We also thank the Instituto Estadual do Ambiente—INEA for the authorization to collect samples in Brejo do Espinho.

The original author names and dates of the foraminifera species found:

Affinetrina sp.
Affinetrina sommeri (Tinoco, 1955).
Ammonia cf. *A. veneta* (Schultze, 1854).
Elphidiella sp.
Trichohyalus sp.
Lachlanella sp.
Quinqueloculina sp.A.
Quinqueloculina seminulum (Linnaeus, 1758).
Miliolinella sp.
Massilina protea (Parcker, 1953).
Neopateoris sp.
Quinqueloculina laevigata d'Orbigny, 1839.
Pseudotriloculina subgranulata (Cushman, 1918).
Rosalina globularis d'Orbigny, 1826.

Triloculina sp.
Pyrgo sp.
Triloculina lutea d'Orbigny, 1839.
Varidentella implexa (Terquem & Terquem, 1886).
Wiesnerella auriculata (Egger, 1893).
Bolivina aenariensis var. *multicostata* Cushman, 1918.
Bulimina marginata d'Orbigny, 1826.
Cassidulina curvata Phleger & Parker, 1951.
Globigerinoides ruber (d'Orbigny, 1839).
Gyroidina umbonata (Silvestre, 1898).
Planulina foveolata (Brady, 1884).
Trifarina bradyi Cushman, 1923.

Appendix A. Supplementary data

Supplementary data to this article can be found online at https://doi.org/10.1016/j.marmicro.2023.102319.

References

Abu-Zied, R.H., Bantan, R.A., 2013. Hypersaline benthic foraminifera from the Shuaiba Lagoon, eastern Red Sea, Saudi Arabia: their environmental controls and usefulness in sea-level reconstruction. Mar. Micropaleontol. 103, 51–67. https://doi.org/10.1016/j.marmicro.2013.07.005.

Al-Dubai, T.A., Abu-Zied, R.H., Basaham, A.S., 2018. Diversity and distribution of benthic foraminifera in the Al-Kharrar Lagoon, eastern Red Sea coast, Saudi Arabia. Micropaleontology. 63 (5), 275–303. https://doi.org/10.47894/mpal.63.5.02.

Amao, A.O., Kaminski, M.A., Babalola, L., 2018. Benthic foraminifera in hypersaline Salwa Bay (Saudi Arabia): an insight into future climate change in the Gulf region? J. Foraminiferal Res. 48 (1), 29–40. https://doi.org/10.2113/gsjfr.48.1.29.

Araujo, J.C., Macario, K.C.D., Moreira, V.N., Passos, A.S., Jesus, P.B., Seoane, J.C.S., Dias, F.F., 2021. Bioindicators of sea-level fluctuations in southeastern Brazil: new data and methodological review. Radiocarbon. 63 (4), 1149–1163. https://doi.org/10.1017/rdc.2021.507.

Areias, C., Spotorno-Oliveira, P., Bassi, D., Iryu, Y., Nash, M., Castro, J.W.A., Tâmega, F. T.S., 2020. Holocene Sea-surface temperatures and related coastal upwelling regime recorded by vermetid assemblages, southeastern Brazil (Arraial do Cabo, RJ). Mar. Geol. 425, 106183 https://doi.org/10.1016/j.margeo.2020.106183.

Areias, C., Barbosa, C.F., Cruz, A.P.S., McKenzie, J.A., Ariztegui, D., Eglinton, T., Haghipour, N., Vasconcelos, C., Sánchez-Román, M., 2022. Organic matter diagenesis and precipitation of Mg-rich carbonate and dolomite in modern hypersaline lagoons linked to climate changes. Geochim. Cosmochim. Acta 37, 14–32. https://doi.org/10.1016/j.gca.2022.09.030.

Bahniuk, A., McKenzie, J., Perri, E., Bontognali, T.R.R., Vogeli, N., Rezende, C.E., Rangel, T.P., Vasconcelos, C., 2015. Characterization of environmental conditions during microbial Mg-carbonate precipitation and early diagenetic dolomite crust formation: Brejo do Espinho, Rio de Janeiro, Brazil. Geol. Soc. Lond. Spec. Publ. 418, 243–259. https://doi.org/10.1144/SP418.11.

Barbiere, E., Coe, N.R., 1999. Spatial and temporal variation of rainfall of the East Fluminense Coast and Atlantic Serra Do Mar, State of Rio de Janeiro, Brazil. In: Knoppers, B., Bidone, E.D., Abrão, J.J. (Eds.), Enviromental Geochemistry of Coastal Lagoon Systems, Rio De Janeiro, Brazil. UFF, Rio de Janeiro, pp. 47–56.

Barbosa, C.F., 1997. Reconstituição paleoambiental de fácies lagunares com base em foraminíferos: o nível do mar no Quaternário Superior na área de Cabo Frio, RJ. PhD Thesis, Geoscience Institute, Universidade de São Paulo.. Available from. http://www.teses.usp.br/teses/disponiveis/44/44136/tde-05012016-155649/.

Barbosa, C.F., Prazeres, M., Ferreira, B.P., Seoane, J.C.S., 2009. Foraminiferal assemblage and reef check census in coral reef health monitoring of East Brazilian margin. Mar. Micropaleontol. 73 (1–2), 62–69. https://doi.org/10.1016/j.marmicro.2009.07.002.

Belart, P., Habib, R., Raposo, D., Clemente, I., Martins, M.V.A., Frontalini, F., Figueiredo, M.S.L., Lorini, M.L., Laut, L., 2019. Seasonal dynamics of benthic foraminiferal biocoenosis in the tropical Saquarema Lagoonal System (Brazil). Estuaries Coast 42, 822–841. https://doi.org/10.1007/s12237-018-00514-w.

Bernhard, J.M., Bowser, S.S., 1992. Bacterial biofilms as a trophic resource for certain benthic foraminifera. Mar. Ecol. Prog. Ser. 83, 263–272. https://doi.org/10.3354/meps083263.

Bernhard, J.M., Sen Gupta, B.K., 1999. Foraminifera of oxygen-depleted environments. In: Gupta, Sen, B.k. (Eds.), Modern Foraminifera. Springer, Dordrecht, pp. 201–216. https://doi.org/10.1007/0-306-48104-9_12.

Bontognali, T.R.R., Vasconcelos, C., Warthmann, R.J., Bernasconi, S.M., Dupraz, C., Strohmenger, C., McKenzie, J.A., 2010. Dolomite formation within microbial mats in the coastal sabkha of Abu Dhabi (United Arab Emirates). Sedimentology. 57, 824–844. https://doi.org/10.1111/j.1365-3091.2009.01121.x.

Bradshaw, J.S., 1957. Laboratory Studies on the Rate of growth of the Foraminifer, Streblus beccarii (Linné) var. tepida (Cushman). J. Paleo. 31 (6), 1138–1147.

Buosi, C., Châtelet, E.C., Cherchi, A., 2012. Benthic foraminiferal assemblages in the current-dominated Strait of Bonifacio (Mediterranean Sea). J. Foraminiferal Res. 42 (1), 39–55. https://doi.org/10.2113/gsjfr.42.1.39.

Burns, S.J., McKenzie, J.A., Vasconcelos, C., 2000. Dolomite formation and biogeochemical cycles in the Phanerozoic. Sedimentology. 47, 49–61. https://doi.org/10.1046/j.1365-3091.2000.00004.x.

Castro, J.W.A., Suguio, K., Seoane, J.C.S., Cunha, A.M., Dias, F.F., 2014. Sea-level fluctuations and coastal evolution in the state of Rio de Janeiro, southeastern Brazil. An. Acad. Bras. Cienc. 86, 671–683. https://doi.org/10.1590/0001376520142014007.

Chronopoulou, P.M., Salonen, L., Bird, C., Reichart, G.J., Koho, K.A., 2019. Metabarcoding Insights into the Trophic Behavior and Identity of Intertidal Benthic Foraminifera. Front. Microbiol. 10, 1169. https://doi.org/10.3389/fmicb.2019.01169.

Clarke, K.R., Gorley, R.N., 2006. PRIMER-E. User Manual/Tutorial: Primer vol. 6. E Ltd., Plymouth (182 pp.).

Clarke, K.R., Somerfield, P.J., Gorley, R.N., 2008. Testing of null hypotheses in exploratory community analyses: similarity profiles and biota-environment linkage. J. Exp. Mar. Biol. Ecol. 366, 56–69. https://doi.org/10.1016/j.jembe.2008.07.009.

Debenay, J.-P., Geslin, E., Eichler, B.B., Duleba, W., Sylvestre, F., Eichler, P., 2001. Foraminiferal assemblages in a hypersaline lagoon, Araruama (R.J.) Brazil. J. Foraminiferal Res. 31 (2), 133–151. https://doi.org/10.2113/0310133.

Delfino, D.O., Wanderley, M.D., Silva e Silva, L.H., Feder, F., Lopes, F.A.S., 2012. Sedimentology and temporal distribution of microbial mats from Brejo do Espinho, Rio de Janeiro. Sediment. Geol. 263, 85–95. https://doi.org/10.1016/j.sedgeo.2011.08.009.

Fatela, F., Taborda, R., 2002. Confidence limits of species proportions in microfossil assemblages. Mar. Micropaleontol. 45, 169–174. https://doi.org/10.1016/S0377-8398(02)00021-X.

Fichtner, V., Schurr, S.L., Strauss, H., Vasconcelos, C., Goetschl, K.E., Oliveira, C.A., Barbosa, C.F., Immenhauser, A., 2023. The Relationship between bacterial sulfur cycling and ca/Mg carbonate precipitation-old tales and new insights from Lagoa Vermelha and Brejo do Espinho, Brazil. Geosciences 13 (8), 229. https://doi.org/10.3390/geosciences13080229.

Geslin, E., Debenay, J.-P., Duleba, W., Bonetti, C., 2002. Morphological abnormalities of foraminiferal tests in Brazilian environments: comparison between polluted and non-polluted areas. Mar. Micropaleontol. 45 (2), 151–168. https://doi.org/10.1016/S0377-8398(01)00042-1.

Giordano, L., Ferraro, L., Salvatore, M., Oscurato, L.S., Maddalena, P., 2019. Morphometric analysis on benthic foraminifera through Atomic Force Microscopy. Mar. Micropaleontol. 153 (101775), 1–9. https://doi.org/10.1016/j.marmicro.2019.101775.

Hayward, B.W., Holzmann, M., Grenfell, H.R., Pawlowski, J., Triggs, C.M., 2004. Morphological distinction of molecular types in Ammonia towards a taxonomic revision of the world's most commonly misidentified foraminifera. Mar. Micropaleontol. 50, 237–271. https://doi.org/10.1016/S0377-8398(03)00074-4.

Hayward, B.W., Holzmann, M., Pawlowski, J., Parker, J.H., Kaushik, T., Toyofuku, M.S., Tsuchiya, M., 2021. Molecular and morphological taxonomy of living Ammonia and related taxa (Foraminifera) and their biogeography. J. Micropalaeontol. 67, 109–313. https://doi.org/10.47894/mpal.67.2-3.01.

Hayward, B.W., Le Coze, F., Vachard, D., Gross, O., 2023. World Foraminifera Database. *Ammonia Veneta* (Schultze, 1854). Accessed at: https://www.marinespecies.org/foraminifera/aphia.php?p=taxdetails&id=738632on2023-11-03.

Hottinger, L., Halicz, E., Reiss, Z., 1993. Recent Foraminifera from the Gulf of Aqaba. Solvenska Akademija Znanosti in Umetnosti, Ljubljana, Red Sea, p. 170.

Jorissen, F.J., Wittling, I., Peypouquet, J.P., Rabouille, C., Relexans, J.C., 1998. Live benthic foraminiferal faunas off Cape Blanc, NW-Africa: Community structure and microhabitats. Deep-Sea Res. I Oceanogr. Res. Pap. 45 (12), 2157–2188. https://doi.org/10.1016/s0967-0637(98)00056-9.

Kaushik, T., Murugan, T., Dagar, S.S., 2019. Morphological variation in the porcelaneous benthic foraminifer Quinqueloculina seminula (Linnaeus, 1758): Genotypes or Morphotypes? A detailed morphotaxonomic, molecular and ecological investigation. Mar. Micropaleontol. 150, 101748 https://doi.org/10.1016/j.marmicro.2019.101748.

Koho, K.A., Lekieffre, C., Nomaki, H., Salonen, I., Geslin, E., Mabilleau, G., Jensen, L.H. S., Reichart, G.J., 2018. Changes in ultrastructural features of the foraminifera Ammonia spp. in response to anoxic conditions: Field and laboratory observations. Mar. Micropaleontol. 138, 72–82. https://doi.org/10.1016/j.marmicro.2017.10.011.

Laut, L.L.M., Martins, V., da Silva, F.S., Crapez, M.A.C., Fontana, L.F., Carvalhal-Gomes, S.B.V., Souza, R.C.C.L., 2016. Foraminifera, Thecamoebians, and Bacterial activity in Polluted Intertropical and Subtropical Brazilian Estuarine Systems. J. Coast. Res. 317, 56–69. https://doi.org/10.2112/jcoastres-d-14-00042.1.

Laut, L., Martins, M.V.A., Frontalini, F., Ballalai, J.M., Belart, P., Habib, R., Fontana, L.F., Clemente, I.M.M.M., Lorini, M.L., Mendonca Filho, J.G., Laut, V.M., Figueiredo, M.S. L., 2017. Assessment of the trophic state of a hypersaline-carbonate environment: Vermelha Lagoon (Brazil). PloS One 12 (9), e0184819. https://doi.org/10.1371/journal.pone.01848 19.

Laut, L., Figueiredo, M.S.L., Lorini, M.L., Belart, P., Clemente, I., Martins, M.V.A., Mendonca Filho, J.G., Laut, V., 2019. Diatoms from the most hypersaline lagoon in Brazil: Vermelha lagoon. Cont. Shelf Res. 181, 111–123. https://doi.org/10.1016/j.csr.2019.05.001.

Laut, L., Belart, P., Carelli, T., Martins, M.V.A., Laut, V., 2022. Insights into the Ecology of Foraminifera from the Most Hypersaline Lagoon in Brazil: Vermelha Lagoon. Estuaries Coast 45, 2632–2649. https://doi.org/10.1007/s12237-022-01073-x.

LeKieffre, C., Spangenberg, J.E., Mabilleau, G., Escrig, S., Meibom, A., Geslin, E., 2017. Surviving anoxia in marine sediments: the metabolic response of ubiquitous benthic foraminifera (Ammonia tepida). PloS One 12 (5), e0177604. https://doi.org/10.1371/journal.pone.0177604.

Leutenegger, S.I., Hansen, H.J., 1979. Ultrastructural and Radiotracer Studies of Pore Function in Foraminifera. Mar. Biol. 54, 11–16. https://doi.org/10.1007/BF00387046.

Levin, L.A., Ekau, W., Gooday, A.J., Jorissen, F., Middelburg, J.J., Naqvi, S.W.A., Rabalais, N.N., Zhang, J., 2009. Effects of natural and human-induced hypoxia on coastal benthos. Biogeosciences. 6, 2063–2098. https://doi.org/10.5194/bg-6-2063-2009.

Loeblich, A.R., Tappan, H., 1988. Foraminiferal Genera and their Classification. Van Nostrand Reinhold, New York. https://doi.org/10.1007/978-1-4899-5760-3, 1059 pp.

Long, M.C., Deutsch, C., Ito, T., 2016. Finding forced trends in oceanic oxygen. Global Bio-geochem Cycles 30, 381–397. https://doi.org/10.1002/2015GB005310.

Lu, W., Barbosa, C.F., Rathburn, A.E., Xavier, P.M., Cruz, A.P.S., Thomas, E., Rickaby, R. E.M., Zhang, Y.G., Lu, Z., 2021. Proxies for paleo-oxygenation: a downcore comparison between benthic foraminiferal surface porosity and I/Ca. Palaeogeogr. Palaeoclimatol. Palaeoecol. 579 (110588) https://doi.org/10.1016/j.palaeo.2021.110588.

McKenzie, J.A., Vasconcelos, C., 2008. Dolomite : the mineral, rock and mountains Origin of the Dolomite Mountains Origin of the dolomite rock Microbial dolomite Microbial - mediated dolomite in the Dolomite Mountains Dolomite Mountains and Triassic sea water chemistry. Sedimentology. 56 https://doi.org/10.1111/j.1365-3091.2008.01027.x.

McKenzie, J.A., Vasconcelos, C., 2010. Linking the geosphere & biosphere to understand dolomite formation. J. Earth Sci. 21, 304–305. https://doi.org/10.1007/s12583-010-0243-5.

Meister, P., McKenzie, J.A., Vasconcelos, C., Bernasconi, S., Frank, M., Gutjahr, M., Schrag, D.P., 2007. Dolomite formation in the dynamic deep biosphere: results from the Peru margin. Sedimentology. 54, 1007–1032. https://doi.org/10.1111/j.1365-3091.2007.00870.x.

Moodley, L., Schaub, B.E.M., van der Zwaan, G.L., Herman, P.M.J., 1998. Tolerance of benthic foraminifera (Protista: Sarcodina) to hydrogen sulphide. Mar. Ecol. Prog. Ser. 169, 77–86. https://doi.org/10.3354/Meps169077.

Moreira da Silva, P.C., 1968. O fenòmeno da ressurgência na costa meridional brasileira. Instituto de Pesquisas da Marinha, Rio de Janeiro 24, 1–31.

Moreira da Silva, P.C., 1973. A ressurgência em Cabo Frio. Instituto de Pesquisas da Marinha, Rio de Janeiro 78, 1–56.

Moreira, N.F., Walter, L.M., Vasconcelos, C., McKenzie, J.A., McCall, P.J., 2004. Role of sulfide oxidation in dolomitization: sediment and pore- water geochemistry of a modern hypersaline lagoon system. Geology. 32 (8), 701–704. https://doi.org/10.1130/G20353.1.

Murray, J.W., 2006. Ecology and Applications of Benthic Foraminifera. Cambridge University Press, New York, pp. 426–429.

Nardelli, M.P., Barras, C., Metzger, E., Mouret, A., Filipsson, H.L., Jorissen, F., Geslin, E., 2014. Experimental evidence for foraminiferal calcification under anoxia. Biogeosciences. 11, 4029–4038. https://doi.org/10.5194/bg-11-4029-2014.

Nascimento, G.S., Eglinton, T.I., Haghipour, N., Albuquerque, A.L., Bahniuk, A., McKenzie, J.A., Vasconcelos, C., 2019. Oceanographic and sedimentological influences on carbonate geochemistry and mineralogy in hypersaline coastal lagoons, Rio de Janeiro state, Brazil. Limnol. Oceanogr. 64, 2605–2620. https://doi.org/10.1002/lno.11237.

O'Malley, B.J., Schwing, P.T., Martínez-Colón, M., Spezzaferri, S., Machain-Castillo, M. L., Larson, R.A., Brooks, G.R., Ruiz-Fernández, A.C., Hollander, D.J., 2021. Development of a benthic foraminifera based marine biotic index (Foram-AMBI) for the Gulf of Mexico: a decision support tool. Ecol. Indic. 120, 106916 https://doi.org/10.1016/j.ecolind.2020.106916.

Petersen, J., Riedel, B., Barras, C., Pays, O., Guihéneuf, A., Mabilleau, G., Schweizer, M., Meysman, F.J.R., Jorissen, F.J., 2016. Improved methodology for measuring pore patterns in the benthic foraminiferal genus Ammonia. Mar. Micropaleontol. 128, 1–13. https://doi.org/10.1016/j.marmicro.2016.08.001.

R Core Team, 2020. R: A Language and Environment for Statistical Computing. R Foundation for Statistical Computing, Vienna, Austria. URL. https://www.R-project.org/.

Raposo, D., Clemente, I., Figueiredo, M., Vilar, A., Lorini, M.L., Frontalini, F., Martins, V., Belart, P., Fontana, L., Habib, R., Laut, L., 2018. Benthic foraminiferal and organic matter compounds as proxies of environmental quality in a tropical coastal lagoon: the Itaipu Lagoon (Brazil). Mar. Pollut. Bull. 129, 114–125. https://doi.org/10.1016/j.marpolbul.2018.02.018.

Rathburn, A.E., Willingham, J., Ziebis, W., Burkett, A.M., Corliss, B.H., 2018. A New biological proxy for deep-sea paleo-oxygen: Pores of epifaunal benthic foraminifera. Sci. Rep. 8 (9456), 1–8. https://doi.org/10.1038/s41598-018-27793-4.

Richirt, J., Bouchet, V.M.P., Schweizer, M., Mouret, A., 2019a. Morphological Distinction of three Ammonia Phylotypes Occurring along European Coasts. J. Foraminiferal Res. 49, 76–93. https://doi.org/10.2113/gsjfr.49.1.76.

Richirt, J., Champmartin, S., Schweizer, M., Mouret, A., Petersen, J., Ambari, A., Jorissen, F.J., 2019b. Scaling laws explain foraminiferal pore patterns. Sci. Rep. 9 (9149), 1–11. https://doi.org/10.1038/s41598-019-45617-x.

Richirt, J., Riedel, B., Mouret, A., Schweizer, M., Langlet, D., Seitaj, D., Meysman, F.J.R., Slomp, C.P., Jorissen, F.J., 2020. Foraminiferal community response to seasonal anoxia in Lake Grevelingen (the Netherlands). Biogeosciences 17, 1415–1435. https://doi.org/10.5194/bg-17-1415-2020.

Richirt, J., Schweizer, M., Mouret, A., Quinchard, S., Saad, S.A., Bouchet, V.M.P., Wade, C.M., Jorissen, F.J. 2021. Biogeographic distribution of three phylotypes (T1, T2 and T6) of Ammonia (foraminifera, Rhizaria) around Great Britain : new insights from combined molecular and morphological recognition, J. Micropalaeontol. 40, 61–74. doi:https://doi.org/10.5194/jm-40-61-2021.

Richirt, J., Guihéneuf, A., Mouret, A., Schweizer, M., Slomp, C.P., Jorissen, F., 2022. A historical record of benthic foraminifera in seasonally anoxic Lake Grevelingen, the Netherlands. Palaeogeogr. Palaeoclimatol. Palaeoecol. 599, 111057 https://doi.org/10.1016/j.palaeo.2022.111057.

Saad, S.A., Wade, C.M., 2016. Biogeographic distribution and habitat association of Ammonia genetic variants around the coastline of Great Britain. Mar. Micropaleontol. 124, 54–62. https://doi.org/10.1016/j.marmicro.2016.01.004.

Sánchez-Román, M., Vasconcelos, C., Schmid, T., Dittrich, M., McKenzie, J.A., Zenobi, R., Rivadeneyra, M.A., 2008. Aerobic microbial dolomite at the nanometer scale: Implications for the geologic record. Geology. 36, 879–882. https://doi.org/10.1130/G25013A.1.

Sánchez-Román, M., Vasconcelos, C., Warthmann, R., Rivadeneyra, M., McKenzie, J.A., 2009. Microbial Dolomite Precipitation under Aerobic Conditions: Results from Brejo do Espinho Lagoon (Brazil) and Culture experiments. In: Eberlig, G.P., McKenzie, J.A. (Eds.), Perspectives in Carbonate Geology. John Wiley & Sons, Ltd, Chichester, West Sussex, UK, pp. 167–178. https://doi.org/10.1002/9781444312065.ch11.

Sanz-Montero, M.E., Cabestrero, Ó., Sánchez-Román, M., 2019. Microbial Mg-rich carbonates in an extreme alkaline lake (Las Eras, Central Spain). Front. Microbiol. 10, 1–15. https://doi.org/10.3389/fmicb.2019.00148.

Sariaslan, N., Langer, 2021. Atypical, high-diversity assemblages of foraminifera in a mangrove estuary in northern Brazil. Biogeosciences. 18, 4073–4090. https://doi.org/10.5194/bg-18-4073-2021.

Schweizer, M., Jauffrais, T., Choquel, C., Méléder, V., Quinchard, S., Geslin, E., 2022. Trophic strategies of intertidal foraminifera explored with single-cell microbiome metabarcoding and morphological methods: what is on the menu? Ecol. Evol. 12 (11), e9437 https://doi.org/10.1002/ece3.9437.

Sen Gupta, B.K., Machain-Castillo, M.L., 1993. Benthic foraminifera in oxygen-poor habitats. Mar. Micropaleontol. 20, 183–201. https://doi.org/10.1016/0377-8398(93)90032-S.

Shiraishi, F., Hanzawa, Y., Asada, J., Cury, L.F., Bahniuk, A.M., 2023. Decompositional processes of microbial carbonates in Lagoa Vermelha, Brazil. J. Sediment. Res. 93, 202–211. https://doi.org/10.2110/JSR.2022.053.

Spadafora, A., Perri, E., McKenzie, J.A., Vasconcelos, C., 2010. Microbial biomineralization processes forming modern Ca:Mg carbonate stromatolites. Sedimentology 57, 27–40. https://doi.org/10.1111/j.1365-3091.2009.01083.x.

Tetard, M., Beaufort, L., Licari, L., 2017. A new optical method for automated pore analysis on benthic foraminifera. Mar. Micropaleontol. 136, 30–36. https://doi.org/10.1016/j.marmicro.2017.08.005.

Tong, H., Feng, D., Peckmann, J., Roberts, H.H., Chen, L., Bian, Y., Chen, D., 2019. Environments favoring dolomite formation at cold seeps: a case study from the Gulf of Mexico. Chem. Geol. 518, 9–18. https://doi.org/10.1016/j.chemgeo.2019.04.016.

Tucker, M.E. (Ed.), 1988. Techniques in Sedimentology. Blackwell Scientific Publications, Oxford, p. 408.

Turcq, B., Martin, L., Flexor, J.-M., Suguio, K., Pierre, C., Tasayaco-Ortega, L., 1999. Origin and evolution of the quaternary coastal plain between Guaratiba and Cabo Frio, State of Rio de Janeiro. In: B. Knoppers, E.D. Bidone, J.J. Abrão (Eds.), Enviromental Geochemistry of Coastal Lagoon Systems, Rio de Janeiro, Brazil. pp. 25–46.

Valentin, J.L., 1984. Analyse des parametrès hydrobiologiques dans la remontée de Cabo Frio (Brésil). Mar. Biol. 82, 259–276. https://doi.org/10.1007/BF00392407.

Van Lith, Y., Vasconcelos, C., Martins, J.C.F., McKenzie, J.A., 2002. Bacterial sulfate reduction and salinity: two controls on dolomite precipitation in Lagoa Vermelha and Brejo do Espinho (Brazil). Hydrobiologia. 485, 35–49. https://doi.org/10.1023/A:1021323425591.

Van Lith, Y., Warthmann, R., Vasconcelos, C., McKenzie, J.A., 2003. Sulphate-reducing bacteria induce low-temperature Ca-dolomite and high Mg-calcite formation. Geobiology. 1 (1), 71–79. https://doi.org/10.1046/j.1472-4669.2003.00003.x.

Vasconcelos, C., McKenzie, J.A., 1997. Microbial mediation of modern dolomite precipitation and diagenesis under anoxic conditions Lagoa Vermelha, Rio de Janeiro, Brazil. Nature. 67 (3), 378–390. https://doi.org/10.1306/D4268577-2B26-11D7-8648000102C1865D.

Vasconcelos, C., Warthmann, R., McKenzie, J.A., Visscher, P.T., Bittermann, A.G., van Lith, Y., 2006. Lithifying microbial mats in Lagoa Vermelha, Brazil: modern Precambrian relics? Sediment. Geol. 185, 175–183. https://doi.org/10.1016/j.sedgeo.2005.12.022.

Vieira, F.S., Koutsoukos, E.A., Machado, A.J., Dantas, M.A.T., 2015. Biofaciological zonation of benthic foraminifera of the continental shelf of Campos Basin, SE Brazil. Quat. Int. 377, 18–27. https://doi.org/10.1016/j.quaint.2014.12.020.

Wang, F., Liu, J., Qiu, J., Wang, H., 2014. Historical evolution of hypoxia in East China Sea off the Changjiang (Yangtze River) estuary for the last ~13,000 years: evidence from the benthic foraminiferal community. Cont. Shelf Res. 90, 151–162. https://doi.org/10.1016/j.csr.2014.02.013.

Warthmann, R., van Lith, Y., Vasconcelos, C., McKenzie, J.A., Karpoff, A.M., 2000. Bacterially induced dolomite precipitation in anoxic culture experiments. Geology. 28 (12), 1091–1094. https://doi.org/10.1130/0091-7613(2000)28<1091:BIDPIA>2.0.CO;2.

Warthmann, R., Vasconcelos, C., McKenzie, J.A., 2005. Lithifying microbial mats in Lagoa Vermelha, Brazil: a model system for Precambrian carbonate formation? Geophys. Res. Abstr. 7, 1630. https://doi.org/10.1016/j.sedgeo.2005.12.022.

Ye, F., Huang, X., Zhang, X., Zhang, D., Zeng, Y., Tian, L., 2012. Recent oxygen depletion in the Pearl River Estuary, South China: geochemical and microfaunal evidence. J. Oceanogr. 68, 387–400. https://doi.org/10.1007/s10872-012-0104-1.